Energetic photons from intermediate energy proton- and heavy-ion-induced reactions

W. Bauer, G. F. Bertsch, W. Cassing, and U. Mosel
Cyclotron Laboratory, Michigan State University, East Lansing, Michigan 48824
and Institut für Theoretische Physik, University of Giessen, 6300 Giessen, Federal Republic of Germany
(Received 6 August 1986)

The cross section for emitting high energy gamma rays in heavy-ion collisions is calculated in a model based on the Boltzmann-Uehling-Uhlenbeck equation. The elementary production cross section is assumed to be neutron-proton bremsstrahlung. Comparison is made with experimental data at bombarding energies from 20 to 84 MeV/nucleon. The calculations are found to roughly reproduce the energy spectrum, bombarding energy dependence, and angular distribution. From the numerical analysis we conclude that the production of high-energy γ rays is limited to the very early stage of the collision.

I. INTRODUCTION

Recent experiments on photon emission in intermediate energy heavy ion collisions show a significant yield of photons with energies above 50 MeV.[1–7] Different mechanisms have been suggested for the emission process, including coherent nucleus-nucleus bremsstrahlung, nucleon bremsstrahlung in the nuclear potential field, and bremsstrahlung from individual proton-neutron collisions. In detailed theoretical calculations, it seems clear that the last mechanism is more important than the first two. Ko *et al.*[8] studied photon production in an intranuclear cascade model and found that the np bremmstrahlung was more important than the coherent bremsstrahlung except for collisions of very heavy nuclei. Nifenecker and Bondorf[9] made an analytic study that came to a similar conclusion. The role of the nuclear potential field was assessed in studies by Bauer *et al.*[10] and by Bertsch and Nakayama.[11] Bauer *et al.* described the dynamics with the time dependent Hartree-Fock (TDHF) method, finding that the potential field bremsstrahlung was an order of magnitude too small to explain the data. In Ref. 11 infinite nuclear matter approximations were applied to show that the np collisional bremsstrahlung had the same order of magnitude as the data, while the potential field bremsstrahlung was negligble. The calculation by Cassing *et al.*[12] took the phase space distribution of nucleons from TDHF dynamics, avoiding the use of nuclear matter approximations. However, this required making some specific assumptions about the time history of the photon production. In both Refs. 11 and 12 it is assumed that only first collisions may produce high energy photons. In contrast, in Ref. 9 the conclusion was reached that more than ten collisions per participant nucleon were needed to explain the data.

It is therefore of interest to examine a model that contains a complete np collisional history of the system, to see when the photons are created, and whether the simple first-collision assumption is valid. The only calculable theory for heavy ion collisions that includes the important physical effects at intermediate bombording energy is given by the Boltzmann-Uehling-Uhlenbeck (BUU) equation. This equation for the evolution of the nucleon phase space density includes mean field as well as collisional dynamics, and contains the effects of the Pauli principle. In this work we will use this theory to answer the questions raised in the preceding paragraph. The numerical method we use is the one introduced in Ref. 13; details of our treatment are discussed in the next section. In later sections we compare to data on proton-induced reactions and heavy ion reactions. The agreement we find for both kinds of reactions gives us confidence to make definite conclusions about the mechanism and time history of the energetic photon production.

II. OUR MODEL

In this paper we conduct a dynamical study of the heavy ion collision process using the Boltzmann-Uehling-Uhlenbeck equation.[13–15] This equation describes the time evolution of the Wigner function $f(\mathbf{r},\mathbf{k},t)$ in phase space.

$$\frac{\partial f_1}{\partial t}+\mathbf{v}\cdot\nabla_r f_1-\nabla_r U\cdot\nabla_p f_1=\frac{4}{(2\pi)^3}\int d^3k_2 d^3k_3 d\Omega\, v_{12}\frac{d\sigma}{d\Omega}\delta^3(\mathbf{k}_1+\mathbf{k}_2-\mathbf{k}_3-\mathbf{k}_4)\times[f_1 f_2(1-f_3)(1-f_4)-f_3 f_4(1-f_1)(1-f_2)]\,. \quad (1)$$

Here $d\sigma/d\Omega$ is the nucleon-nucleon reaction cross section, v_{12} is the relative velocity of the colliding nucleons, and U is the mean field potential which we parametrize as

$$U(\rho)=-218\ \text{MeV}\,\rho/\rho_0+164\ \text{MeV}\,(\rho/\rho_0)^{4/3}\,. \quad (2)$$

This potential reproduces nuclear matter saturation properties and has a nuclear compressibility of $\kappa=235$ MeV. Equation (1) is solved using the pseudoparticle simulation with 100 test particles per nucleon. Numerical and technical details are described, for example, in Ref. 15.

The elementary process for the photon production is assumed to be

$$p+n \rightarrow p+n+\gamma \ . \tag{3}$$

For the description of the elementary cross section we adopt the hard-sphere collision limit from Ref. 16, modified as in Ref. 12 to allow for energy conservation.

$$\frac{d^2\sigma^{\text{elem}}}{dE_\gamma d\Omega_\gamma} = \alpha \frac{R^2}{12\pi} \frac{1}{E_\gamma} (2\beta_f^2 + 3\sin^2\theta_\gamma \beta_i^2) \ . \tag{4}$$

Here R is the radius of the sphere, α is the fine structure constant, and β_i and β_f are the initial and final velocity of the proton in the proton-neutron center of mass system.

With $R^2=3$ fm^2 this formula fits the proton-deuteron data of Edgington and Rose[17] reasonably well (compare Fig. 2). We should stress that it is not the main goal of this paper to give a realistic and detailed microscopic theoretical formulation of the free process in Eq. (3). Our primary interest is focused on the medium corrections to this cross section in heavy ion collisions and on the time scale for γ production. In Ref. 12 we proposed that energetic photons are a very sensitive probe for the momentum and energy distribution of the nucleons at the early stages of the collision. We want to follow this suggestion more accurately in this paper.

One obtains the double differential photon cross section for heavy-ion collisions in the nucleus-nucleus c.m. system from the double differential cross section for the elementary process (3) in the individual p-n c.m. system taking medium corrections into account via

$$\frac{d^2N(b)}{dE_\gamma d\Omega_\gamma} = \sum_{\text{p-n coll}} \int \frac{d\Omega_e}{4\pi} \frac{E_\gamma}{E'_\gamma} \frac{1}{\sigma_{\text{NN}}} \frac{d^2\sigma^{\text{elem}}}{dE'_\gamma d\Omega'_\gamma} (\mathbf{k}_1-\mathbf{k}_2) \times [1-f(\mathbf{r},\mathbf{k}_3,t)][1-f(\mathbf{r},\mathbf{k}_4,t)] \ , \tag{5a}$$

where $\mathbf{r}$ and t give the space-time coordinates of each collision. We integrate over impact parameter to obtain the total yield

$$\frac{d^2\sigma^{\text{eff}}}{dE_\gamma d\Omega_\gamma} = \int d^2b \frac{d^2N(b)}{dE_\gamma d\Omega_\gamma} \ . \tag{5b}$$

Here $\mathbf{k}_1$ and $\mathbf{k}_2$ are the momenta of the incoming proton and neutron and $\mathbf{k}_3$ and $\mathbf{k}_4$ are the momenta of the outgoing proton and neutron. σ_{NN} is the total nucleon-nucleon cross section and taken to be 30 mb. In Eq. (5a) the probability for emitting a photon in a single collision of a proton and a neutron is given by

$$\frac{1}{\sigma_{\text{NN}}} \frac{d^2\sigma^{\text{elem}}}{dE'_\gamma d\Omega'_\gamma}$$

in the individual p-n c.m. system. $N(b)$ is the number of emitted photons in the heavy ion collision as a function of impact parameter b which is implicitly contained in the Wigner function f.

Using nonrelativistic kinematics the final momenta are determined by the initial momenta for a given photon momentum via

$$\mathbf{k}_3 = \tfrac{1}{2}\mathbf{K} + \tfrac{1}{2}(4mE-K^2)^{1/2}\hat{\mathbf{e}} \ , \tag{6a}$$

$$\mathbf{k}_4 = \tfrac{1}{2}\mathbf{K} - \tfrac{1}{2}(4mE-K^2)^{1/2}\hat{\mathbf{e}} \ , \tag{6b}$$

where m is the nucleon mass and $\mathbf{K}$ and E are given by

$$\mathbf{K} = \mathbf{k}_1 + \mathbf{k}_2 - \mathbf{k}_\gamma \tag{7}$$

and

$$E = (k_1^2 + k_2^2)/2m - E_\gamma \ . \tag{8}$$

$\hat{\mathbf{e}}$ is a unit vector. In Eq. (5) the integration $d\Omega_e$ is performed over the two angular components of $\hat{\mathbf{e}}$ which are not determined by energy and momentum conservation.

The term

$$[1-f(\mathbf{r},\mathbf{k}_3,t)][1-f(\mathbf{r},\mathbf{k}_4,t)]$$

represents the effects of Pauli blocking of the final state phase space. The Wigner distribution functions $f(\mathbf{r},\mathbf{k},t)$ are obtained using the BUU prescription. The reliability of the results obtained in our approach depends critically on the adequate description of the Pauli blocking of the final phase space. To test the quality of our method, we use the following setup (cf. Fig. 1).

A proton with momentum $\mathbf{k}_1=(0.5,0,0)$ GeV/c collides with a neutron with momentum $\mathbf{k}_2=(-0.25,0,0)$ GeV/c inside a nucleus. It is assumed that a photon is emitted in the y direction with a given energy E_γ. Depending on E_γ we evaluate the function

$$\Pi(\mathbf{k}_1,\mathbf{k}_2,\mathbf{k}_\gamma) = \frac{1}{4\pi} \int d\Omega_e [1-f(\mathbf{r},\mathbf{k}_3,t)][1-f(\mathbf{r},\mathbf{k}_4,t)] \ . \tag{9}$$

This function has a value of 0 for events with a completely blocked final phase space and a value of 1 for events which are completely unblocked. For this test we use a phase space distribution $f(\mathbf{r},\mathbf{k},t)$ obtained from a BUU simulation of a mass 50 nucleus.

In Fig. 1 we show the result of our test. $\Pi(\mathbf{k}_1,\mathbf{k}_2,\mathbf{k}_\gamma)$ is plotted as a function of E_γ (circles). It can be seen that Π decreases smoothly with increasing E_γ. This is to be expected since $(\mathbf{k}_1+\mathbf{k}_2)/2$ lies inside the Fermi sphere of the nucleus. One can also calculate the values of Π analytically in this simple test case, if one assumes sharp Fermi

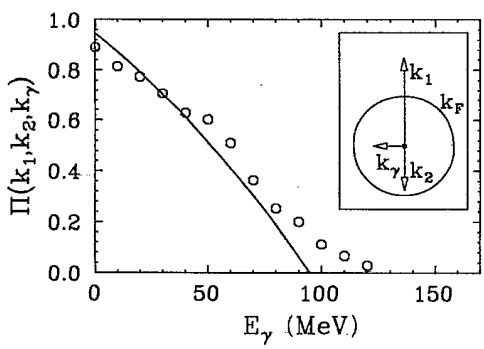

FIG. 1. Comparison of the Pauli-blocking prescription used in the numerical calculations (circles) with the analytic result for a sharp Fermi sphere.

spheres without finite size corrections for the momentum distribution of the nucleus. The result of such a calculation is represented by the solid line in Fig. 1. It can be seen that both calculations agree quite well up to γ energies of 80–90 MeV. From 90 MeV up to the kinematical threshold the function Π shows some deviations from the analytic calculation with the infinite nuclear matter assumptions. Therefore caution should be used at photon energies around the kinematical threshold. We will discuss this from case to case while comparing our results to the experimental data. However, since this test case invokes momenta typical for the heavy ion collisions investigated in our study, and our results show only small fluctuations around the smooth curve, we feel confident that Pauli blocking is taken into account with a reasonable degree of accuracy up to photon energies of the order of 80–90 MeV.

III. COMPARISON TO PROTON-NUCLEUS DATA

First we compare our results to proton-nucleus data. From the standpoint of our model this is a much easier problem than a heavy ion collision. In the case of a proton-nucleus reaction the incoming proton has a fixed momentum which is given by the beam energy. The neutron has a momentum given by the ground state momentum distribution of the nucleus. Unlike the situation in heavy ion collisions, the momentum distribution of the nucleus will not get distorted very much during the course of the proton-nucleus reaction.

In Fig. 2 we compare the results of our calculation for 140 MeV proton-nucleus collisions to the data of Edgington and Rose[17] for deuterium, aluminum, and carbon targets. We view this comparison as a test for the right magnitude of our elementary photon production cross section (4). For the case of deuterium we made the simplifying assumption that the neutron is at rest in the laboratory frame. We then only calculate the p-n photon production cross section using Eq. (4). For the Al and C targets we use the BUU code to simulate the dynamical process, taking the medium corrections of the p-nucleus system into account.

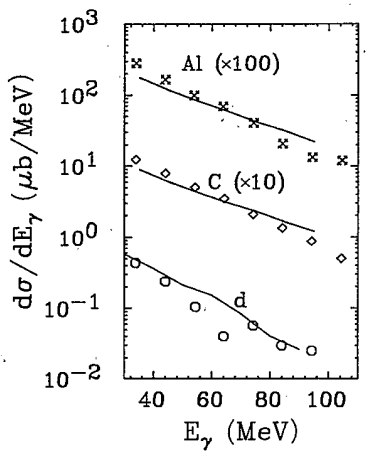

FIG. 2. Photon cross section $d\sigma/dE_\gamma$ for the reaction 140 MeV proton + nucleus. The data are taken from Ref. 17.

The fact that our calculated spectra are slightly flatter than the experimental ones for p + C and p + Al could be an indication for the limits of accuracy of our prescription for Pauli blocking. But, since we obtain good agreement for all targets and photon energies, we conclude that our fit of the elementary production cross section has a reasonable degree of accuracy.

IV. DYNAMICAL EVOLUTION OF THE HEAVY ION COLLISION

Before presenting the photon cross sections for heavy ion collisions, we will briefly describe the evolution of the phase space density for the BUU equation. Figure 3 shows contour plots of the time evolution of the phase space density for a $^{12}C + {}^{12}C$ collision at a beam energy of 40 MeV per nucleon. The beam direction is along the z axis. Displayed is

$$F(z,k_z,t)=\int dx\,dy\,dk_x\,dk_y f(x,y,z,k_x,k_y,k_z,t)\ . \qquad (10)$$

$F(z,k_z,t)$ is the phase space distribution as a function of longitudinal spatial coordinate and momentum integrated over all transversal momenta and spatial coordinates. The impact parameter for this simulation is 0 fm (central collision). Nucleon-nucleon collisions are switched off in this simulation to show the distortion effects of the mean field on the phase space distribution (cf. also Ref. 18).

We see that the nucleons in the interpenetrating region are not appreciably accelerated, so the momentum distribution from the initial state provides a reasonable approximation to the distribution in the overlapping zone. However, there is a channel of low phase space density between the two nuclei that remains during the early stages of the reaction. The appearance of this channel is a very important dynamical effect in this BUU calculation. Colliding nucleons which produce a high energy photon will preferably scatter into this region of phase space. The added available phase space for the nucleons after an inelastic γ-producing collision will increase the photon yield con-

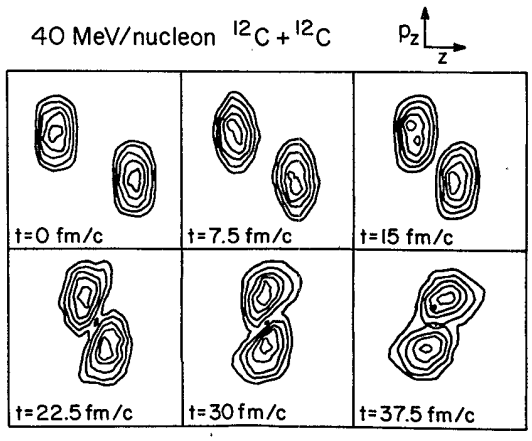

FIG. 3. Contour plots of the time evolution of the phase space density $f(\mathbf{r},\mathbf{k},t)$ as a function of longitudinal coordinate and momentum for a ^{12}C-^{12}C collision at a beam energy of 40 MeV/nucleon. Displayed is an area of length 20 fm in the z direction and 1 GeV/c in the p_z direction. The contour lines correspond to cuts at values of 0.1, 0.3, 0.5, 0.7, and 0.9 for f.

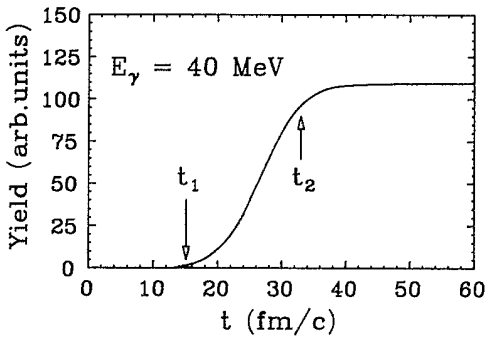

FIG. 4. Photon yield as a function of time for a ^{12}C-^{12}C collision at a beam energy of 40 MeV/nucleon. At $t_1=15$ fm/c the nuclei touch in coordinate space and at $t_2=33$ fm/c the maximum overlap is reached.

siderably compared to a calculation in which two intersecting Fermi spheres are used to describe the momentum distributions. We speculate that this is the reason we obtain larger cross sections than in Ref. 11.

When nucleon-nucleon collisions are turned on in the BUU calculation, the phase space channel is quickly filled by collisions in the early stages of the reaction. This effect reduces the available final state phase space for photon producing proton-neutron collisions in later stages of the nucleus-nucleus collision considerably. In addition, nucleon-nucleon collisions depopulate the high momentum tails of the momentum distribution which are primarily responsible for the production of high energy photons. Both effects together cause the high energy photons as well as pions[19] to be produced in the early stage of the heavy ion collision.

In Fig. 4 we show the yield of 40 MeV photons from a 40 MeV/nucleon ^{12}C + ^{12}C collision as a function of time. This diagram can be compared to Fig. 3 for the time scales involved. At $t_1=15$ fm/c the nuclei just merely touch in coordinate space, and at $t_2=33$ fm/c the nuclei have maximum overlap. Between these two marks practically all high energy photons are produced, whereas there is no yield added to the photon production in later stages of the heavy ion collision. This result supports the first collision approaches: High energy photons are produced in the early stages of heavy ion collisions. It is one of the most important results of our present study, since it means that high energy photons are probes of the momentum and energy distribution of nucleons in heavy ions in early stages of the heavy ion collision as proposed in earlier publications.[10,12]

V. IMPACT PARAMETER DEPENDENCE

It is also possible to obtain information on the impact parameter dependence of the photon yield in our model. Since we assume proton-neutron collisions to be the elementary production process, one would naively expect the yield of photons to be proportional to the geometric overlap of target and projectile.

In Fig. 5(a) we display the impact parameter dependence of the number of p-n collisions and the yield of 50

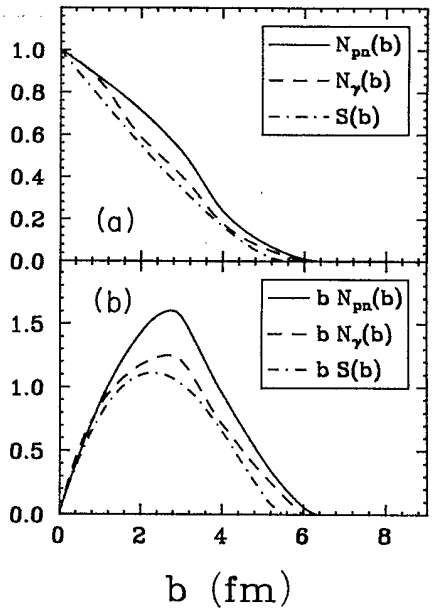

FIG. 5. (a) Impact parameter dependence of the number of p-n collisions (solid line), the photon yield (dashed line), and the geometrical overlap area of two circles (dot-dashed line). All curves are normalized to 1 at $b=0$ fm. (b) The same functions weighted with the impact parameter b.

MeV photons for a ^{12}C + ^{12}C collision at a beam energy of 84 MeV/nucleon. Both curves are normalized to 1 at $b=0$ fm to show their scaling behavior with impact parameters; the actual number of collisions at $b=0$ fm is 19 for this reaction. If the photon yield would scale exactly like the number of proton-neutron collisions with impact parameter, both curves, $N_{pn}(b)$ and $N_\gamma(b)$, would be identical. But we observe that for large impact parameters N_γ is smaller than N_{pn}. This is essentially due to the fact that only smaller momentum components and consequently less energetic nucleons are available at the surface of the nuclei as compared to the interior. This effect is even more visible in Fig. 5(b), where N_γ and N_{pn} have been weighted with the impact parameter.

In order to compare the impact parameter dependence of N_γ with the result of simple geometrical considerations we have also plotted the function

$$S(b)=[2R^2\cos^{-1}(b/2R)-b(R^2-b^2/4)^{1/2}]/\pi R^2$$

in Fig. 5. $S(b)$ is the geometrical overlap between two circles of radius $R=R(^{12}\mathrm{C})$, again normalized to 1 at $b=0$ fm. From the comparison of $S(b)$ and $N_\gamma(b)$ we conclude that the impact parameter dependence of the yield of high energy photons can be approximated by the impact parameter dependence of the overlap area of two circles as in Ref 12.

VI. NUCLEUS-NUCLEUS DATA

We compare our calculations to recent measurements by Grosse *et al.*[1] and Stevenson *et al.*[4] We have concentrated on lighter systems (^{14}N + ^{12}C, ^{12}C + ^{12}C), because our calculations are computionally quite time consuming.

We are able to obtain double differential high energy photon cross sections and thus can compare angular distributions as well as energy spectra to experiment.

In Fig. 6 we compare the results of our calculations to energy spectra from Refs. 1 and 4. The three lower curves represent the results from N + C collisions at 40 (squares), 30 (circles), and 20 (diamonds) MeV/nucleon beam energy. The upper curve is the result of a C + C collision at 84 MeV/nucleon beam energy (octagons). Displayed is the cross section for photons emitted at an angle $\theta = 90°$ with respect to the beam axis.

We generally overpredict the N + C data of Stevenson *et al.*[4] This effect increases with decreasing beam energy. While our results at 40 MeV/nucleon are only a factor of ≈ 1.5 higher than the experimental data, we overpredict the experiment by a factor between 3 and 8 for the beam energy of 20 MeV/nucleon. On the other hand, we see that our calculation lies a factor of ≈ 1.5 below the 84 MeV/nucleon $^{12}C + {}^{12}C$ data of Grosse *et al.*[1] Just looking at Fig. 6, it appears as if our calculation would show the wrong beam energy dependence. However, in Fig. 7 we have plotted the beam energy dependence of the total high energy photon production cross section for photons in the energy range of 50–100 (upper curve) and 100–150 (lower curve) MeV in the center of mass frame for a $^{12}C + {}^{12}C$ collision. The corresponding data points (octagons and diamonds) are taken from Ref. 1. It is clear from this figure that we are able to reproduce the beam energy dependence of the data of Grosse *et al.* For all beam energies our calculations are a factor between 1.5 and 2 lower than the data for high energy photons in the energy range between 50 and 100 MeV.

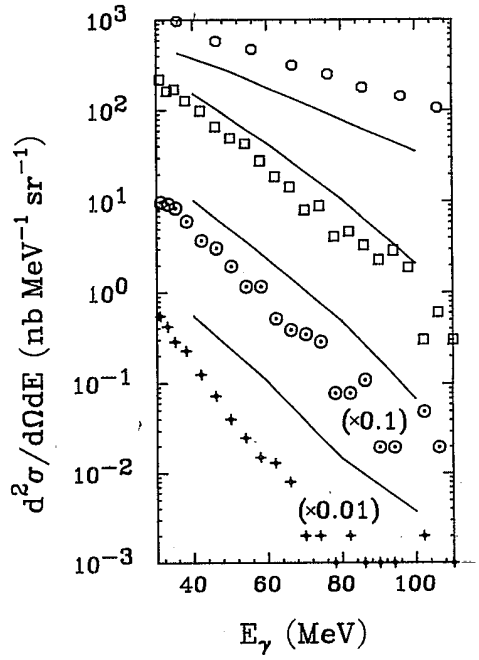

FIG. 6. Photon energy spectra from heavy ion collisions. The solid lines are the results of our calculations and the symobls represent the experimental data from Refs. 1 and 4. The emission angle of the photon is always 90° with respect to the beam axis. Circles: 84 MeV/nucleon $^{12}C + {}^{12}C$; squares: 40 MeV/nucleon $^{14}N + {}^{12}C$; circles with central point: 30 MeV/nucleon $^{14}N + {}^{12}C$; diamonds: 20 MeV/nucleon $^{14}N + {}^{12}C$.

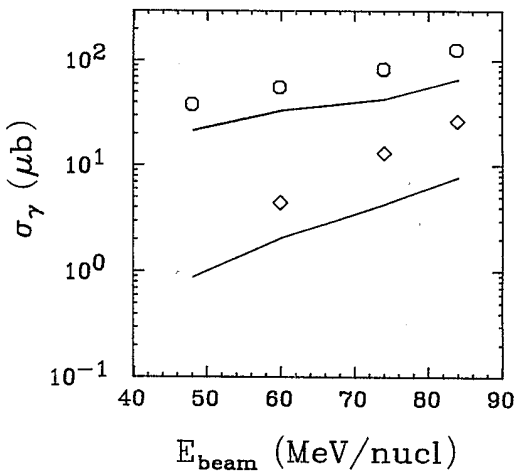

FIG. 7. Beam energy dependence of the photon yield for photons of energy 50–100 MeV (upper curve, octagons) and 100–150 MeV (lower curve, diamonds). The data are taken from Ref. 1 and represented by the symbols. Our calculations are represented by solid lines.

It appears to us that the data of Stevenson *et al.* and Grosse *et al.* show beam energy dependences which are not fully compatible. Therefore further experimental study is needed to clarify the situation.

We compare our angular distributions of high energy photons to experimental data from Stevenson *et al.*[4] and Grosse *et al.*[1] In Fig. 8 the double differential photon

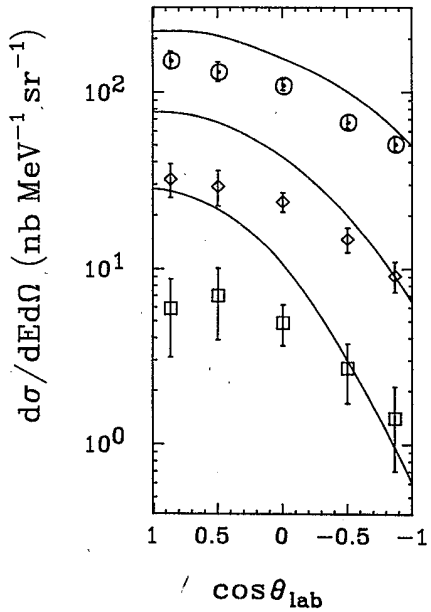

FIG. 8. Comparison of our calculation to the photon angular distributions measured by Stevenson *et al.* (Ref. 3) for a 40 MeV $^{12}N + {}^{12}C$ collision in the laboratory frame and photon energies of 40 (circles), 60 (diamonds), and 80 (squares) MeV.

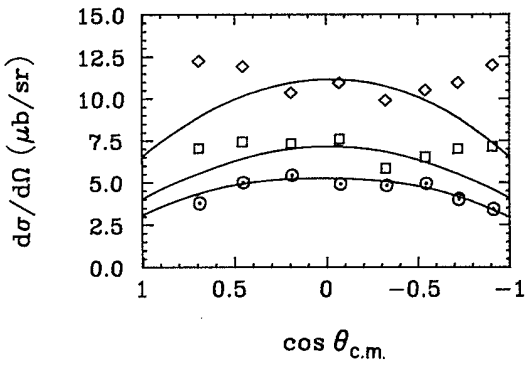

FIG. 9. Comparison of our calculation to the photon angular distribution measured by Grosse *et al.* (Ref. 1) for photons of energy between 50 and 100 MeV in the center of mass frame and beam energies of 84 (diamonds), 74 (squares), and 60 (circles) MeV/nucleon. Our calculations (solid lines) have been uniformly scaled up by a factor of 1.8 for ease of comparison.

cross sections for photon energies 40 MeV (circles), 60 MeV (diamonds), and 80 MeV (squares) are shown in the laboratory system for a $^{14}N + {}^{12}C$ collision at a beam energy of 40 MeV/nucleon. While our results are in excellent agreement with the data for a gamma energy of 40 MeV, we see large deviations (up to a factor of 4) from the data at forward angles for the higher gamma energies.

The large variation in the angular distribution for the higher energies in our calculation is largely due to the transformation from the center of mass frame to the laboratory frame. Therefore it is useful to compare theoretical predictions to the experimental angular distributions in the center of mass frame. In Fig. 9 we plot the experimental data of Grosse *et al.*[1] for the differential cross section for photons with an energy between 50 and 100 MeV in the center of mass system. The diamonds correspond to $E_{\text{beam}}=84$ MeV/nucleon, the squares to 74 MeV/nucleon, and the circles to 60 MeV/nucleon. Also displayed are our corresponding theoretical predictions. As already mentioned before, our results usually underpredict the data of Grosse *et al.* slightly. To make the comparison easier we therefore have scaled all our results in Fig. 9 up by a factor of 1.8. It can be seen that the data follow our calculation exactly for the beam energy of 60 MeV/nucleon. The agreement is still very good for the 74 MeV data, but at 84 MeV the experimental distribution is closer to isotropy than we predict. These deviations are slightly bigger than the experimental error bars which we did not include in Fig. 9 and which are typically 2 μb/sr for the 84 MeV data. Overall however, the experimental angular distributions of Grosse *et al.* are in reasonable agreement with our theory.

Even though our angular distribution for the elementary process as given by Eq. (4) is essentially of dipolar shape, the angular distributions of photons from heavy ion collisions are rather flat due to the angular smearing of the Fermi motion of the colliding proton-neutron pair.

In all of these comparisons with experiment one has to keep in mind the following points. Firstly, we have used a formula for the elementary production process, (4), which is derived under very simplifying assumptions. It is quite possible that this formula does not describe the beam energy dependence of the high energy gamma cross section accurately enough. Another point which has been made earlier in this paper is that our prescription for the Pauli blocking mechanism is model independent only for photon energies up to 80% of the kinematical threshold.

A last point is that our model uses a quasiclassical approximation of the nuclear momentum and energy distribution of the nucleons. In the rest frame of a single nucleus only momenta up to the Fermi momentum are available. Thus our momentum distributions lack the quantum tails. For this reason we do not feel comfortable enough to make predictions for photon energies larger than 100 MeV in the beam energy range under investigation in this paper.

VII. CONCLUSION AND OUTLOOK

We conclude from our study that the source of high energy photons in heavy ion reactions is bremsstrahlung from individual proton-neutron collisions. The angular distributions and energy spectra of the photons observed experimentally in heavy ion collisions are reproduced in our calculations with a reasonable accuracy.

Since we perform a dynamical study of the heavy ion collision process, we are able to learn about the time scales of energetic photon production. It turns out that high energy γ rays are produced in the early stage of the reaction before maximum overlap of projectile and target is reached. This is a very important piece of information, since it qualifies high energy photons as probes of the momentum and energy distributions of nucleons in the early stages of heavy ion collisions. The latter conclusion is quite independent of our assumption for the elementary production cross section from Eq. (4).

Correlation experiments between photons and, for example, protons emitted in heavy ion collisions would be helpful to confirm the production mechanism and should give us deeper insight into the momentum and energy distributions of nucleons in heavy ions during the nonequilibrium phase of nucleus-nucleus reactions.

ACKNOWLEDGMENTS

One of the authors (U.M.) gratefully acknowledges the generous hospitality of the Michigan State University Cyclotron Laboratory. Support for this work was as follows: W.B. by the Studienstiftung des Deutschen Volkes; G. B. and U.M. by the National Science Foundation under Grant PHY 85-19653. This work was supported by Bundesministerium für Forschung und Technologie and Gesellschaft für Schwerionenforschung Darmstadt.

[1]E. Grosse, P. Grimm, H. Heckwolf, W. F. J. Mueller, H. Noll, A. Oskarson, H. Stelzer, and W. Roesch, Europhys. Lett. 2, 9 (1986).

[2]N. Herrmann, J. Albinski, R. Bock, E. P. Feng, R. Freifelder, A. Gobbi, P. Grimm, E. Grosse, K. D. Hildenbrand, H. T. Liv, W. F. J. Mueller, H. Stelzer, P. Braun-Munzinger, J. Stachel, P. R. Maurenzig, A. Olmi, and A. A. Stefanini, Gesellschaft für Schwerionenforschung Annual Report 1985, p. 86.

[3]H. Heckwolf, Gesellschaft für Schwerionenforschung Report 86-3, 1986.

[4]J. Stevenson, K. B. Beard, W. Benenson, J. Clayton, E. Kashy, A. Lampis, D. J. Morrissey, M. Samuel, R. J. Smith, C. L. Tam, and J. S. Winfield, Phys. Rev. Lett. 57, 555 (1986).

[5]H. Nifenecker, M. Kwato Njock, M. Maurel, E. Monnand, J. Pinston, F. Schussler, D. Barneoud, C. Guet, and Y. Schutz, in Proceedings of the XIV International Winter Meeting on Nuclear Physics, Bormio, 1986, p. 239.

[6]K. Beard, W. Benenson, C. Bloch, E. Kashy, J. Stevenson, D. J. Morrissey, J. van der Plicht, B. Sherrill, and J. S. Winfield, Phys. Rev. C 32, 1111 (1985).

[7]N. Alamanos, P. Braun-Munzinger, R. F. Freifelder, P. Paul, J. Stachel, T. C. Awes, R. L. Ferguson, F. E. Obenshain, F. Plasil, and G. R. Young, Phys. Lett. **173B**, 392 (1986).

[8]C. M. Ko, G. Bertsch, and J. Aichelin, Phys. Rev. C **31**, 2324 (1985).

[9]H. Nifenecker and J. P. Bondorf, Nucl. Phys. **A442**, 478 (1985).

[10]W. Bauer, W. Cassing, U. Mosel, M. Tohyama, and R. Y. Cusson, Nucl. Phys. **A456**, 159 (1986).

[11]K. Nakayama and G. Bertsch, Michigan State University Report 563, 1986.

[12]W. Cassing, T. Biro, U. Mosel, M. Tohyama, and W. Bauer, Phys. Lett. B (in press).

[13]G. Bertsch, H. Kruse, and S. das Gupta, Phys. Rev. C **29**, 675 (1984).

[14]H. Kruse, B. Jacak, and H. Stoecker, Phys. Rev. Lett. **54**, 289 (1985).

[15]J. Aichelin and G. Bertsch, Phys. Rev. C **31**, 1730 (1985).

[16]J. D. Jackson, *Classical Electrodynamics* (Wiley, New York, 1962), p. 733.

[17]J. A. Edgington and B. Rose, Nucl. Phys. **89**, 523 (1966).

[18]W. Cassing, in *Coincident Particle Emission from Continuum States in Nuclei,* edited by H. Machner and P. Jahn (World Scientific, Singapore, 1984), pp. 340—376.

[19]W. Cassing, in *Phase Space Approach to Nuclear Dynamics,* edited by M. Di Toro (World Scientific, Singapore, 1986), pp. 64—93.